CRYSTAL GROWTH & DESIGN

pubs.acs.org/crystal

Article

Investigation of Structure−Property Relationships of Three Nitroaromatic Compounds: 1-Fluoro-2,4,6-trinitrobenzene, 2,4,6-Trinitrophenyl Methanesulfonate, and 2,4,6-Trinitrobenzaldehyde

Dominik E. Dosch,[†] Marco Reichel,[†] Max Born,[†] Thomas M. Klapötke,* and Konstantin Karaghiosoff

Cite This: https://dx.doi.org/10.1021/acs.cgd.0c01049

Read Online

ACCESS | Metrics & More | Article Recommendations | Supporting Information

ABSTRACT: Recently the investigation of the correlation between the crystal structure and important properties such as the sensitivity and thermostability of energetic materials has gained more and more interest among experts in the field. To contribute to this development, several models for the sensitivity prediction of energetic materials have been applied to the title compounds. Very often, older models that focus on bond dissociation enthalpy or electrostatic potential result in values that differ significantly from values of actual measurements. However, more recent models such as Hirshfeld surface analysis and fingerprint plot analysis offer an improved correlation between prediction and practical tests. We compared these methods with the aforementioned older models and gained further insight into the structure−property relationships of energetic materials. The accuracy of predictions of structure−property relationships that can be deduced from a crystal structure increases with the sample size over time. Therefore, this method should be pursued and applied to different energetic materials in the future, for a better understanding of those relationships.

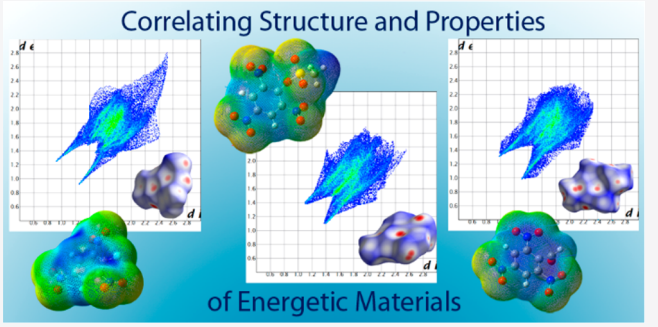

INTRODUCTION

In 1997 Spackmann communicated a novel concept for the definition and visualization of a molecule in a crystal based on Hirshfeld's Stockholder partitioning scheme.[1,2] This method for crystal analysis and crystal engineering was further refined and became famous as the Hirshfeld surface in 1998.[3] In 2002 McKinnon and Spackmann complemented their method with a 2D fingerprint plot analysis for improved visualization of intermolecular close contacts in a crystal.[4] This work was followed by the initial development of the Crystal Explorer software in 2004 and 2005, which has been continuously improved since then.[5] With the current version of Crystal Explorer various interactions in the crystal can be easily visualized and quantified, including features such as crystal surface mapping and close contact analysis, which make it a valuable tool for crystal engineering and material design.[6] In 2014, Hirshfeld surface and fingerprint plot analysis found their way into the analysis and development of energetic materials for the first time.[7] Since then various authors such as Gozin,[8] Klapötke,[9] and Shreeve[10] have utilized this methodology and the Crystal Explorer software for the investigation and design of new energetic materials with the goal of achieving a deeper insight into structure−property relationships, especially with regard to sensitivity and thermal stability. With regard to the synthesis and design of new energetic materials, insensitivity toward external stimuli is one of the most important requirements among other characteristics such as improved environmental compatibility, higher density, and thermal stability as well as increased detonation velocity and pressure.[11,12] One strategy to achieve an increased performance of HEDMs is to use compounds with a high heat of formation, but this is often related to a higher sensitivity toward external stimuli.[13] Due to this contrary behavior,[13−15] the molecular design and the crystallographic design have to be considered in the creation of new materials, to achieve a suitable balance between safety and performance.[10] For this purpose, we applied a combination of various methods to all of the title compounds, which form a group of 1-substituted derivatives of 2,4,6-trinitrobenzene. Those molecules are interesting building blocks for the synthesis of more sophisticated energetic materials and serve as model compounds for an analysis of structure−property relationships. The applied set of methods comprises both preceding predictive models such as the computation of BDE and ESP values and newer methods such as Hirshfeld surface and fingerprint plot analysis.[7−10,16] By comparing the results of different prediction models with experimental values, we hope

Received: July 29, 2020
Revised: December 2, 2020

to achieve a better understanding of the energetic behavior regarding the aforementioned compounds and also a deeper insight into the structure−property relationships of energetic materials in general.

RESULTS AND DISCUSSION

Spectroscopic Characterization. The three title compounds were prepared by utilizing modified and optimized methods and intensely characterized by multinuclear NMR spectroscopy, vibrational spectroscopy (IR, Raman), and elemental analysis as well as single-crystal X-ray diffraction. The ^{1}H NMR chemical shifts found for aromatic protons (**1**, 9.20 ppm; **2**, 9.24 ppm; **3**, 9.16 ppm) are in good agreement with other known 1-substituted trinitrobenzene derivatives such as TNT (8.8 ppm) and picric acid (9.0 ppm).[17,18] The ^{13}C{^{1}H} NMR spectra reveal corresponding chemical shifts between 120 and 190 ppm. Compound **1** shows two distinct signals for the nitro groups in ortho and para positions in the ^{14}N NMR spectrum. In the case of molecules **2** and **3**, no distinct signals for the nitro groups were found due to the rather large signal widths of 440 and 500 Hz. Typical Raman and infrared vibration modes were found in the corresponding spectra and assigned according to the available literature (Table 1).[19]

Table 1. Characteristic Vibration Modes of 1−3[a]

	1		2		3	
	IR	Raman	IR	Raman	IR	Raman
ν(C−H)	3063	3063	3095	3097	3096	3104
ν_{as}(NO_2)	1541	1548	1543	1547	1554	1553
ν_{s}(NO_2)	1342	1364	1343	1363	1343	1351
ν(C−N)	923	940	919	1089	919	938
δ(NO_2)	737	817	730	823	729	826

[a] $\nu_{as/s}$, asymmetric/symmetric vibration mode; δ, deformation vibration.

All three compounds show very similar values for the symmetric, asymmetric, and deformation modes of the nitro groups. The same applies to the C−H and C−N modes of the three title compounds, with the exception of the Raman C−N mode of compound **2**. It has been previously shown by other researchers that the bond dissociation enthalpy (BDE) can be directly linked to the sensitivity of energetic materials (Figure 1).[20,21] All three compounds are expected to have very similar

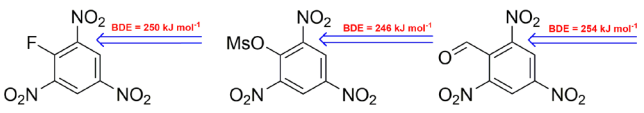

Figure 1. Calculated BDE values of the weakest bond in molecules **1**−**3**, considering all X−C bonds (X = C, O, N, F).

BDE values and therefore similar sensitivities toward external stimuli using this particular model. In this work, the BDEs were calculated on the basis of the respective crystal structure data and the B3LYP/6-311G+(d,p) method. According to various studies, the BDE of a molecule can be considered as the most important factor in pyrogenic decomposition. The BDE correlates to a trigger bond which is first to break and can therefore be utilized to assess the sensitivity of a material.[10]

The C−N bond of the *o*-nitro group was identified as the weakest bond in all of the investigated compounds. All BDE values of compounds **1**−**3** fall in a range between those of RDX (161 kJ mol^{-1}) and TATB (355 kJ mol^{-1}), which is the reason for categorizing them as sensitive.[15,22−28] The calculation-based trend of BDEs is **2** < **1** < **3**, but the relative difference is very small (<10 kJ mol^{-1}). On the basis of this model, very similar sensitivity values would be expected. The electrostatic potential (ESP) can be utilized for the visualization of the bond strength inside a molecule and therefore as an indicator for the potential sensitivity (Figure 2).[11] In addition, the calculation of h_{50} values or the acquisition of *volume-based sensitivities* based on ESP is possible.[11]

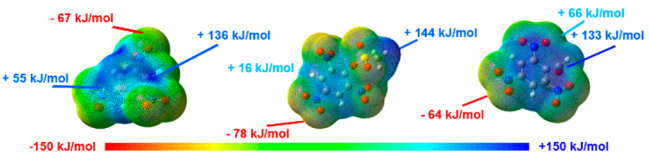

Figure 2. ESPs of **1** (left), **2** (center), and **3** (right), calculated on the 0.02 electron bohr^{3} hypersurface.

Regarding the ESP, all compounds show a significantly larger surface area in the positive range and the corresponding values are more pronounced in comparison to peak values of negative areas. This distribution and the strongly positive center of the investigated compounds is a typical indicator for sensitive materials.[26−28] The differences between the peak positive spot and the peak negative spot (**1**, +69 kJ mol^{-1}; **2**, +66 kJ mol^{-1}; **3**, +69 kJ mol^{-1}) are very similar for all three compounds. Therefore, a similar behavior toward external stimuli is expected.

Structure−Property Relationship. Impact and friction resemble external mechanical stimuli which can cause the displacement of stabilizing layers in the crystal and therefore lead to internal strains. If the strain energy is below the lowest BDE, the integrity of the molecule is not affected. In contrast, if the strain energy surpasses the energy necessary to break the weakest bond, the compound will decompose.[7] In addition to the stacking and gearings of the individual layers, the strain caused by an interlayer slide also depends on other stabilizing interactions in the crystal: i.e., hydrogen bridges.[29]

The three isolated molecules **1**−**3** (Figure 3a−c) all show an almost planar benzene ring. When the largest torsion angles of the ortho nitro groups (1: 41, 2: 45, and 3: 41°) are compared, a very similar twisting behavior can be identified. This can be explained by steric effects as well as by electronic repulsion between the substituents at the 1-position and the neighboring nitro groups. Despite those similarities, each compound exhibits a unique packing behavior in the unit cell of the crystal (Figure 3d−f) and therefore a difference in the gearing of the individual layers. Compound **1** exhibits a wavelike pattern with a moderate gearing between each layer. Compound **3** exhibits a wavelike pattern with a higher gearing of the individual layers, and compound **2** shows a layered structure with the lowest gearing of all investigated materials. For compound **3** the strain energy arising from mechanical stimuli is assumed to be the highest due to the high interlayer gearing and therefore the highest sensitivity is expected. Compound **2** exhibits the highest interlayer distance, and therefore this material is expected to be the least sensitive toward mechanical stimuli, as it allows an easier sliding of

https://dx.doi.org/10.1021/acs.cgd.0c01049
Cryst. Growth Des. XXXX, XXX, XXX−XXX

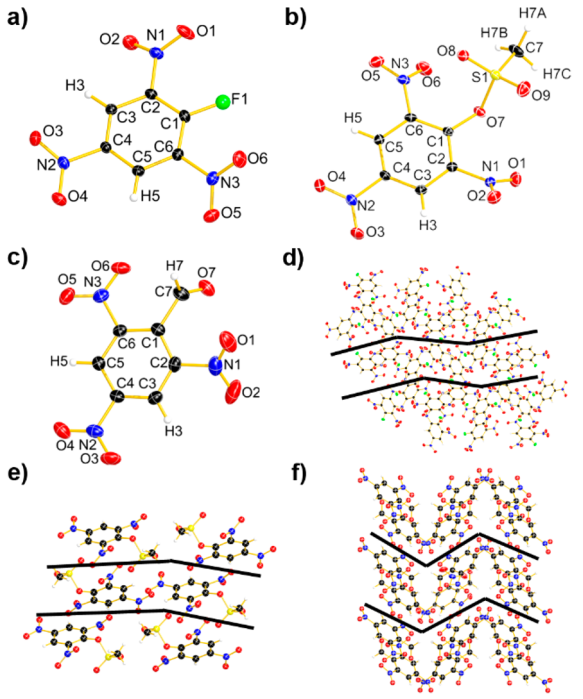

Figure 3. Single-crystal X-ray structures of **1** (a), **2** (b), and **3** (c) and the crystal packing of **1** (d), **2** (e), and **3** (f).

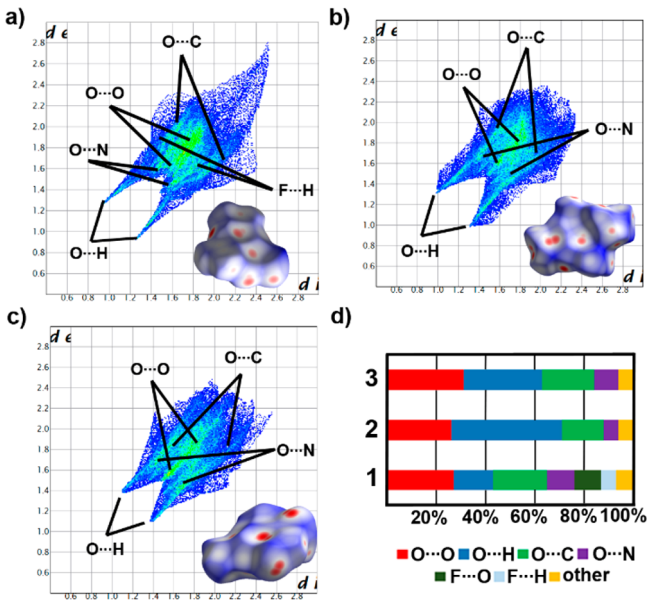

Figure 4. Two-dimensional fingerprint plots in crystal stacking as well as the corresponding Hirshfeld surfaces (bottom right in the 2D plot) of **1** (a), **2** (b), and **3** (c). Color coding: white, distance *d* equals the VDW distance; blue, *d* exceeds VDW distance; red, distance *d* is smaller than the VDW distance. Population of close contacts of **1**−**3** in crystal stacking (d).

adjacent layers without negative oxygen−oxygen repulsions or other detrimental interactions. When this effect is very pronounced, the slip barrier can be reduced significantly enough to become smaller than the bond dissociation energy.[7] Next to crystal packing, a significant contribution to the extent of the slide barrier is made up by intermolecular interactions, which therefore directly correlate with the sensitivity of a compound toward mechanical stimuli. In general, insensitive molecules exhibit a Hirshfeld surface in which the plane features the most red dots representing close contacts and fewer red dots between the individual layers.[29] Compounds **1**−**3** exhibit red dots and therefore close contacts which point out of the molecular plane (Figure 4) and can therefore be considered sensitive. Because none of these close contacts is arranged in a slidable plane, interlayer repulsion results from external stimuli, which is characteristic for sensitive materials.

The experimental sensitivity values for compounds **1**−**3** (IS, 9−10 J; FS, >360 N; ESD, 50−160 mJ) are very similar, and the same would be expected for the distribution and intensity of stabilizing and destabilizing close contacts in the Hirshfeld surface and fingerprint plot analysis of the crystal structures. The compounds show a 3D network with regard to their close contacts, represented by red dots on the surface in all three dimensions, which is typical for sensitive materials. The analysis of the 2D fingerprint plots shows very interesting results, as the distributions and intensities of the close contacts in the model compounds are very different. Less sensitive energetic materials are often designated by numerous and/or strong O···H and N···H interactions, as they facilitate more rigid interlayers, which absorb energy more easily and are hence less likely to cause a detrimental sliding of the planes that induces a repulsion of these layers.[10] Compound **1** shows very few O···H contacts (22%) in comparison to compounds **2** (45%) and **3** (32%), but the number of strong O···H contacts (<2.5 Å) is significantly higher for compound **1**. Apparently, the very few but strong O···H close contacts in compound **1** are capable of stabilizing the molecule to the same extent as significantly more but weaker interactions in compounds **2** and **3**, as they show very similar sensitivities toward external stimuli. The stabilizing N···H close contacts can be neglected in all three cases, as their occurrence is low (0−0.9%) and they can be regarded as weak (>3 Å). The same is true for the stabilizing F···H interactions (1.3%) in compound **1**. The O···O interaction is a particularly important close contact interaction, as a high occurrence of O···O contacts implies a high sensitivity. An increased exposure of nitro groups on the molecular surface causes the risk of explosion to rise due to the increased repulsion in the case of interlayer sliding.[7,10,15,29] The title compounds show significant amounts of O···O close contacts (26−32%) and can therefore be considered sensitive. All O···N and C···N contacts are very weak (>3 Å), which is typical for sensitive materials.[29] The 2D fingerprint plots exhibit two pronounced spikes that indicate strong O···H bonding in all investigated compounds.[10] With respect to d_i + d_e (d_i, distance between the Hirshfeld surface to the nearest atom interior; d_e, distance from the Hirshfeld surface to the nearest atom exterior) the trend for the amount of hydrogen bonds is **2** > **3** > **1**, but an inverse trend is found for the relative strength of the H bonds. These results indicate that not only the quantity but also the relative bond strength for stabilizing interactions must be considered when utilizing Hirshfeld surface and fingerprint plot analysis for the sensitivity assessment of energetic materials.

Heat of Formation and Detonation Parameters. The performance of an energetic material depends directly on its density, which therefore is not only a decisive factor but most interestingly results from the packing behavior within the crystal. We observed the crystal densities of **1**−**3** to be 1.89, 1.84, and 1.76 g cm^{-3} at 145 K, respectively. Hence, the calculated densities under ambient conditions are 1.84, 1.80, and 1.72 g cm^{-3}. To calculate the heat of formation (HOF),

https://dx.doi.org/10.1021/acs.cgd.0c01049
Cryst. Growth Des. XXXX, XXX, XXX−XXX

extremely precise theoretical methods must be applied, since experimental values are often inaccurate.[10] The calculation of the HOF was therefore performed using ab initio calculations which make use of the optimized molecule geometry obtained by refining the obtained geometry from the X-ray diffraction experiment. According to Trouton's rule, the HOF is determined by the subtraction of the sublimation enthalpy from the HOF of the corresponding gas-phase species.[11] To obtain the HOF of the corresponding gas-phase species, the atomization energies were subtracted from the total enthalpy of the molecules.[30,31] All calculations were carried out on a CBS-4M level of theory in combination, starting from the respective crystal structures. On application of the specific densities and the EXPLO5 (V6.05)[32] thermochemical code, the detonation properties of **1**−**3** were determined and are given in Table 2. They were calculated at the Chapman−Jouguet (C-J) point with the help of the stationary detonation model using a modified Becker−Kistiakowski−Wilson state equation for the system. The C-J point was found by the Hugoniot curve of the system by its first derivative.[32,33]

Table 2. Physical and Calculated Detonation Parameters of Compounds 1−3 Using the EXPLO5 Computer Code

	1	2	3
formula	$C_6H_2N_3O_6F$	$C_7H_5N_3O_9S$	$C_7H_3N_3O_7$
M_r (g mol^{-1})	231.09	307.19	241.11
IS[a] (J)	10	9	10
FS[b] (N)	>360	>360	>360
ESD (mJ)	160	50	120
N[c] (%)	18.18	13.68	17.43
N + O[d] (%)	59.72	60.55	63.88
Ω_{CO_2}[e] (%(	−48.5	−39.1	−56.4
T_{melt}[f] (°C)	126.7	139.4	101.6
T_{dec}[g] (°C)	350.6	237.4	185.1
$\rho_{25\,°C}$[h] (g cm)	1.837	1.795	1.721
ΔH_f^o[i](kJ mol^{-1})	−532.8	−386.1	−163.2
	EXPLO5 V 6.05		
ΔU_f^o[j] (kJ kg^{-1})	−4070	−3904	−4391
$T_{C\text{-}J}$[k] (K)	3301	2240	3361
$P_{C\text{-}J}$[l] (GPa)	23.8	12.6	20.4
V_{det}[m] (ms^{-1})	7376	5863	7062
V_0[n] (dm^3 kg^{-1})	606.9	383.9	616.1

[a]Impact sensitivity.[22] [b]Friction sensitivity.[23] [c]Nitrogen content. [d]Combined nitrogen and oxygen contents. [e]Absolute oxygen balance assuming the formation of CO or CO_2. [f]Melting point from DTA. [g]Decomposition from DTA. [h]Calculated room-temperature density. [i]Heat of formation calculated at the CBS-4M level of theory for FMN, experimentally determined for MN. [j]Detonation energy. [k]Detonation temperature. [l]Detonation pressure. [m]Detonation velocity. [n]Colume of detonation gases under standard temperature and pressure conditions.

The HOFs of the compounds are in the order **3** > **1** > **2**, while the densities are in the order **1** > **2** > **3**. According to these results, similar values for the detonation pressure and the detonation velocity can be expected. However, the mesyl substituent in compound **2** leads to a significantly lowered oxygen balance in comparison to the other two compounds. It also exhibits significantly lower values for V_{det} and $P_{C\text{-}J}$. With regard to these values, compounds **1** and **3** slightly exceed those of TNT (6881 m s^{-1}, 18.9 GPa), while molecule **2** is unable to compete.[26−28]

CONCLUSIONS

1-Fluoro-2,4,6-trinitrobenzene, 2,4,6-trinitrophenyl methanesulfonate, and 2,4,6-trinitrobenzaldehyde have been prepared and intensely characterized. The molecular structures of all the aforementioned compounds were elucidated by single-crystal X-ray diffraction. Older methods for the prediction of an energetic material's sensitivity (BDE, ESP) were compared with newer, current methods which are based on the crystal structure of a compound (Hirshfeld surface and fingerprint plot analysis). We found that a combination of very few but strong stabilizing interactions in a crystal may result in the same sensitivity as numerous but significantly weaker stabilizing interactions. Another key result is the fact that all investigated energetic materials had at least 25% of destabilizing O···O interactions as well as close contacts between the individual layers. The broader application of Hirshfeld surface analysis could lead to a deeper insight and understanding of the relationship between structure and sensitivity of an energetic material. Sensitivity values could be predicted or even determined without the need to prepare large amounts of an energetic material. This is not only environmentally friendly but also leads to a significant increase in safety. Calculations using the EXPLO5 code showed that the performance of the investigated compounds decreases from **1** over **3** to **2**. Except for the last compound, the values are comparable to those of TNT.

EXPERIMENTAL SECTION

General Information. 1-Fluoro-2,4-dinitrobenzene, pyridine, iodine *N*,*N*-dimethyl-p-nitrosoaniline, methanesulfonic anhydride, perchloric acid, nitric acid, sulfuric acid, oleum, and potassium nitrate are commercially available. Potassium picrate and TNT were used from a group internal stockpile.

For NMR spectroscopy the solvent DMSO-d_6 was dried using 3 Å molecular sieves. Spectra were recorded on a Bruker Avance III spectrometer operating at 400.1 MHz (^{1}H), 100.6 MHz (^{13}C), and 28.9 MHz (^{14}N). Chemical shifts are referred to TMS (^{1}H, ^{13}C) and $MeNO_2$ (^{14}N). Raman spectra were recorded with a Bruker MultiRam FT Raman spectrometer using a neodymium-doped yttrium aluminum garnet (Nd:YAG) laser (λ = 1064 nm) with a power of 1074 mW. The samples for infrared spectroscopy were placed under ambient conditions onto an ATR unit using a PerkinElmer Spectrum BX II FT-IR system spectrometer. Melting and/or decomposition points were detected with a OZM DTA 552-Ex instrument. The scanning temperature range was set from 293 to 673 K at a scan rate of 5 K min^{-1}. Elemental analysis was performed with a Vario EL instrument and a Metrohm 888 Titrando device.

Caution! All of the investigated compounds are explosives, which show partially increased sensitivities toward various stimuli (e.g., higher temperatures, impact, friction, and electrostatic discharge). Therefore, proper safety precautions (safety glasses, Kevlar gloves, and earplugs) have to be applied while synthesizing and handling the described compounds.

1-Fluoro-2,4,6-trinitrobenzene. 1-Fluoro-2,4-dinitrobenzene (13.6 g, 72.9 mmol) was slowly added to a nitration mixture consisting of 61.9 mL of sulfuric acid, 50.8 mL of oleum (65%), and potassium nitrate (42.0 g, 415.4 mmol) at 0 °C. The reaction mixture was then stirred for 15 min at 0 °C and subsequently warmed to room temperature before the solution was finally heated to 125 °C for 5 days. The obtained suspension was cooled to ambient temperature and afterward poured onto 750 mL of ice−water. The solid was collected by suction filtration and washed with water (3 × 200 mL) until the filtrate ran clear. The filter cake was dried and recrystallized from boiling tetrachlorocarbon to afford the product upon cooling as pale yellow crystals (9.7 g, yield 57%).

https://dx.doi.org/10.1021/acs.cgd.0c01049
Cryst. Growth Des. XXXX, XXX, XXX−XXX

^{1}H NMR (chloroform-*d*, 400 MHz): δ 9.20 (d, 2H, $^{4}J_{FH}$ = 5.6 Hz) ppm. ^{13}C{^{1}H} NMR (chloroform-*d*, 100 MHz): δ 154.2 (d, $^{1}J_{FC}$ = 292.0 Hz), 142.4 (s, broad), 139.4 (s, broad), 125.9 (d, $^{3}J_{FC}$ = 0.8 Hz) ppm. ^{14}N NMR (chloroform-*d*, 29 MHz): δ −24 (s, NO_2) ppm. ^{19}F NMR (chloroform-*d*, 377 MHz): δ −113.2 (t, $^{4}J_{FH}$ = 5.6 Hz) ppm. IR (ATR, cm^{-1}): $\tilde{\nu}$ 3110 (w), 3089 (w), 3063 (m), 2887 (w), 1620 (s), 1541 (vs), 1482 (m), 1421 (m), 1342 (vs), 1319 (s), 1280 (m), 1258 (m), 1202 (m), 1089 (s), 948 (w), 938 (m), 923 (s), 827 (vw), 776 (w), 757 (w), 737 (s), 718 (s), 709 (vs), 672 (m), 649 (s), 551 (m), 519 (m), 481 (w), 462 (w), 406 (w). Raman (1064 nm, 1000 mW, 25 °C, cm^{-1}): $\tilde{\nu}$ 3063 (9), 2643 (2), 1621 (14), 1548 (36), 1364 (100), 1347 (51), 1279 (14), 1187 (4), 1090 (6), 940 (11), 927 (7), 826 (21), 817 (12), 741 (3), 522 (2), 377 (5), 354 (8), 333 (20), 313 (7), 205 (26), 149 (8), 105 (48), 90 (40). Anal. Calcd for $C_6H_2FN_3O_6$: C, 31.18; H, 0.87; F, 8.22; N, 18.18; O, 41.54. Found: C, 31.42; H, 1.13; N, 18.23. DTA: 127 °C (mp), 351 °C (dec). IS: 10 J. FS: >360 N. ESD: 160 mJ.

2,4,6-Trinitrophenyl Methanesulfonate. Potassium picrate (10.0 g, 37.4 mmol, 1.0 equiv) was suspended in 200 mL of toluene. Methanesulfonic anhydride (6.5 g, 37.4 mmol, 1.0 equiv) was added to the yellow suspension in small portions. After perchloric acid (60% solution in acetic acid, 10 drops) was added, the reaction mixture was stirred for 4 h at 120 °C with a $CaCl_2$-filled drying tube on top of the reflux condenser. After cooling to room temperature, the yellowish byproduct potassium mesylate was separated by filtration and the filter residue was washed with ∼150 mL of toluene. The yellow filtrate phases were combined, and the solvent was removed *in vacuo*. The resulting yellow-orange oil was treated with ∼15 mL of ice-cold ether to precipitate the solid product. The solvents were removed *in vacuo*, and a pale yellow solid was obtained. It was recrystallized from 150 mL of chloroform to afford the product as a white solid (8.6 g, yield 75%).

^{1}H NMR (acetone-d_6, 400 MHz): δ 9.24 (s, 2H), 3.69 (s, 3H) ppm. ^{13}C{^{1}H} NMR (acetone-d_6, 100 MHz): δ 146.3, 145.8, 138.8, 126.0, 40.4 ppm. ^{14}N NMR (acetone-d_6, 29 MHz): δ −22 (s, NO_2) ppm. IR (ATR, cm^{-1}): $\tilde{\nu}$ 3095 (w), 2163 (w), 2004 (w), 1614 (w), 1543 (m), 1373 (m), 1343 (s), 1243 (m), 1192 (m), 1169 (m), 1087 (w), 969 (w), 919 (m), 847 (s), 823 (m), 792 (m), 775 (s), 730 (s), 716 (s), 668 (s), 634 (m), 560 (m), 536 (s), 505 (s). Raman (1064 nm, 1000 mW, 25 °C, cm^{-1}): $\tilde{\nu}$ 3097 (18), 3035 (15), 2942 (46), 1616 (55), 1547 (42), 1363 (100), 1245 (50), 1089 (25), 823 (31), 636 (37), 565 (21), 367 (23), 330 (33), 250 (17). Anal. Calcd for $C_7H_5N_3O_9S$: C, 27.37; H, 1.64; S, 10.44; N, 13.68; O, 46.87. Found: C, 27.34; H, 1.69; N, 13.60; S, 10.99. DTA: 139 °C (mp), 237 °C (dec). IS: 9 J. FS: >360 N. ESD: 50 mJ.

2,4,6-Trinitrobenzaldehyde. Trinitrotoluene (10.0 g, 44.0 mmol, 1 equiv) and *N*,*N*-dimethyl-*p*-nitrosoaniline (7.0 g, 47.0 mmol, 1.1 equiv) were dissolved in 15 mL of pyridine with 50 mg of iodine as a catalyst. The mixture was stirred for 7 days at 20−25 °C. The organic solid was separated by filtration and washed with cold acetone. The obtained crude product was dried *in vacuo* and then dissolved in 180 mL of aqueous HCl (36%) and stirred at 80 °C for 2 h. The product was then separated by filtration and washed acid-free with water. This way 6.4 g (yield 61%) of pure TNBA could be obtained as a black solid.

^{1}H NMR (DMSO-d_6, 400 MHz): δ 10.55 (s, 1H), 9.16 (s, 2H) ppm. ^{13}C{^{1}H} NMR (DMSO-d_6, 100 MHz): δ 188.1, 148.1, 147.7, 134.2, 124.7 ppm. ^{14}N (DMSO-d_6, 29 MHz): δ −20 (s, NO_2) ppm. IR (ATR, cm^{-1}): $\tilde{\nu}$ 3096 (w), 2916 (vw), 1714 (m), 1605 (m), 1554 (s), 1535 (vs), 1452 (w), 1405 (w), 1343 (vs), 1194 (m), 1185 (w), 1157 (m), 1075 (w), 979 (w), 935 (w), 919 (m), 839 (m), 826 (m), 772 (m), 742 (m), 729 (s), 701 (m), 570 (w), 538 (w), 475 (w), 435 (m). Raman (1064 nm, 1000 mW, 25 °C, cm^{-1}): $\tilde{\nu}$ 3104 (8), 2911 (7), 2903 (8), 1713 (16), 1623 (15), 1553 (29), 1382 (32), 1351 (81), 1274 (10), 1197 (12), 981 (8), 938 (7), 842 (13), 826 (18), 334 (22), 292 (8), 255 (7), 232 (19), 203 (34), 192 (26), 151 (36), 88 (100). Anal. Calcd for $C_7H_3N_3O_7$: C, 34.87; H, 1.25; N, 17.43. Found: C, 34.87; H, 1.38; N, 17.12. DTA: 102 °C (mp), 185 °C (dec). IS: 10 J. FS: 360 N. ESD: 120 mJ.

X-ray Measurements. 1-Fluoro-2,4,6-trinitrobenzene and 2,4,6-trinitrobenzaldehyde were dissolved in ethyl acetate, and single crystals were obtained after slow solvent evaporation. Single crystals of 2,4,6-trinitrophenyl methanesulfonate were obtained after slow solvent evaporation of chloroform. Data collection was performed with an Oxford Xcalibur3 diffractometer with a CCD area detector, equipped with a multilayer monochromator, a Photon 2 detector, and a rotating-anode generator, for data collection using Mo Kα radiation (λ= 0.7107 Å). Data collection and reduction were carried out using the CrysAlisPro software.[34] The structures were solved by direct methods (SIR-2014),[35] refined (SHELXLE)[36] by full-matrix least squares on F^2 (ShelxL),[37,38] and finally checked using the PLATON software[39] integrated in the WinGX software suite.[40] The non-hydrogen atoms were refined anisotropically, and the hydrogen atoms were located and freely refined. All Diamond 3 plots are shown with thermal ellipsoids at the 50% probability level; hydrogen atoms are shown as small spheres of arbitrary radius.

■ ASSOCIATED CONTENT

Supporting Information

The Supporting Information is available free of charge at https://pubs.acs.org/doi/10.1021/acs.cgd.0c01049.

^{1}H, ^{13}C, ^{19}F, and ^{14}N NMR spectra, crystallographic information, and detonation parameter calculations (output files) (PDF)

Accession Codes

CCDC 2016174−2016176 contain the supplementary crystallographic data for this paper. These data can be obtained free of charge via www.ccdc.cam.ac.uk/data_request/cif, or by emailing data_request@ccdc.cam.ac.uk, or by contacting The Cambridge Crystallographic Data Centre, 12 Union Road, Cambridge CB2 1EZ, UK; fax: +44 1223 336033.

■ AUTHOR INFORMATION

Corresponding Author

Thomas M. Klapötke − *Department of Chemistry, Ludwig Maximilian University of Munich, D-81377 Munich, Germany;* orcid.org/0000-0003-3276-1157; Email: tmk@cup.uni-muenchen.de

Authors

Dominik E. Dosch − *Department of Chemistry, Ludwig Maximilian University of Munich, D-81377 Munich, Germany;* orcid.org/0000-0003-4804-6473

Marco Reichel − *Department of Chemistry, Ludwig Maximilian University of Munich, D-81377 Munich, Germany;* orcid.org/0000-0003-0137-4816

Max Born − *Department of Chemistry, Ludwig Maximilian University of Munich, D-81377 Munich, Germany*

Konstantin Karaghiosoff − *Department of Chemistry, Ludwig Maximilian University of Munich, D-81377 Munich, Germany;* orcid.org/0000-0002-8855-730X

Complete contact information is available at: https://pubs.acs.org/10.1021/acs.cgd.0c01049

Author Contributions

†D.E.D., M.R., and M.B. contributed equally to this work.

Notes

The authors declare no competing financial interest.

■ ACKNOWLEDGMENTS

Financial support of this work by Ludwig-Maximilian University (LMU), the Office of Naval Research (ONR)

under grant no. ONR.N00014-16-1-2062, and the Strategic Environmental Research and Development Program (SERDP) under contract no. WP19-1287 is gratefully acknowledged. The authors also thank Dr. Teresa Küblböck for her help with the graphics and F-Select GmbH for the generous donation of fluoro chemicals.

REFERENCES

(1) Hirshfeld, F. L. Bonded-atom fragments for describing molecular charge densities. *Theoretica chimica acta* **1977**, *44*, 129−138.
(2) Spackman, M. A.; Byrom, P. G. A novel definition of a molecule in a crystal. *Chem. Phys. Lett.* **1997**, *267*, 215−220.
(3) McKinnon, J. J.; Mitchell, A. S.; Spackman, M. A. Hirshfeld Surfaces: A New Tool for Visualising and Exploring Molecular Crystals. *Chem. - Eur. J.* **1998**, *4*, 2136−2141.
(4) Spackman, M. A.; McKinnon, J. J. Fingerprinting intermolecular interactions in molecular crystals. *CrystEngComm* **2002**, *4*, 378−392.
(5) McKinnon, J. J.; Spackman, M. A.; Mitchell, A. S. Novel tools for visualizing and exploring intermolecular interactions in molecular crystals. *Acta Crystallogr., Sect. B: Struct. Sci.* **2004**, *60*, 627−668.
(6) McKinnon, J. J.; Jayatilaka, D.; Spackman, M. A. Towards quantitative analysis of intermolecular interactions with Hirshfeld surfaces. *Chem. Commun.* **2007**, 3814−3816.
(7) Ma, Y.; Zhang, A.; Xue, X.; Jiang, D.; Zhu, Y.; Zhang, C. Crystal Packing of Impact-Sensitive High-Energy Explosives. *Cryst. Growth Des.* **2014**, *14*, 6101−6114.
(8) Li, H.; Zhang, L.; Petrutik, N.; Wang, K.; Ma, Q.; Shem-Tov, D.; Zhao, F.; Gozin, M. Molecular and Crystal Features of Thermostable Energetic Materials: Guidelines for Architecture of "Bridged" Compounds. *ACS Cent. Sci.* **2020**, *6*, 54−75.
(9) Reichel, M.; Dosch, D.; Klapötke, T.; Karaghiosoff, K. Correlation between Structure and Energetic Properties of Three Nitroaromatic Compounds: Bis(2,4-dinitrophenyl) Ether, Bis(2,4,6-trinitrophenyl) Ether, and Bis(2,4,6-trinitrophenyl) Thioether. *J. Am. Chem. Soc.* **2019**, *141*, 19911−19916.
(10) Zhang, J.; Zhang, Q.; Vo, T. T.; Parrish, D. A.; Shreeve, J. Energetic Salts with π-Stacking and Hydrogen-Bonding Interactions Lead the Way to Future Energetic Materials. *J. Am. Chem. Soc.* **2015**, *137*, 1697−1704.
(11) Klapötke, T. M. *Chemie der hochenergetischen Materialien*, 1st ed.; De Gruyter: Berlin, 2009.
(12) Gao, H.; Shreeve, J. Azole-Based Energetic Salts. *Chem. Rev. (Washington, DC, U. S.)* **2011**, *111*, 7377.
(13) Zhi, C. Y.; Cheng, X. L.; Zhao, F. The Correlation between Electric Spark Sensitivity of Polynitroaromatic Compounds and Their Molecular Electronic Properties. *Propellants, Explos., Pyrotech.* **2010**, *35*, 555.
(14) Thottempudi, V.; Gao, H.; Shreeve, J. Trinitromethyl-substituted 5-nitro- or 3-azo-1,2,4-triazoles: synthesis, characterization, and energetic properties. *J. Am. Chem. Soc.* **2011**, *133*, 6464.
(15) Tang, Y.; Zhang, J.; Mitchell, L. A.; Parrish, D. A.; Shreeve, J. Taming of 3,4-Di(nitramino)furazan. *J. Am. Chem. Soc.* **2015**, *137*, 15984−15987.
(16) Spackman, M. A.; Jayatilaka, D. Hirshfeld surface analysis. *CrystEngComm* **2009**, *11*, 19.
(17) Hussain, I.; Tariq, M. I.; Siddiqui, H. L. Structure Elucidation of Chromogen Resulting from Jaffes's Reaction. *J. Chem. Soc. Pak.* **2009**, *31*, 937.
(18) Soojhawon, I.; Lokhande, P. D.; Kodam, K. M.; Gawai, K. R. Biotransformation of nitroaromatics and their effects on mixed function oxidase system. *Enzyme Microb. Technol.* **2005**, *37*, 527.
(19) Lewis, I. R.; Daniel, N. W.; Griffiths, P. R. Interpretation of Raman Spectra of Nitro-Containing Explosive Materials. Part I: Group Frequency and Structural Class Membership. *Appl. Spectrosc.* **1997**, *51*, 1854.
(20) Li, J. Relationships for the Impact Sensitivities of Energetic C-Nitro Compounds Based on Bond Dissociation Energy. *J. Phys. Chem. B* **2010**, *114*, 2198.
(21) Li, J. A quantitative relationship for the shock sensitivities of energetic compounds based on X−NO_2 (X = C, N, O) bond dissociation energy. *J. Hazard. Mater.* **2010**, *180*, 768.
(22) *Standardization Agreement 4489 (STANAG 4489), Explosives, Impact Sensitivity Tests*; NATO: Brussels, Belgium, 1999.
(23) *Standardization Agreement 4487 (STANAG 4487), Explosives, Friction Sensitivity Tests*; NATO: Brussels, Belgium, 2002.
(24) www.reichel-partner.com.
(25) Test methods according to: *UN Manual of Tests and Criteria, Recommendations on the Transport of Dangerous Goods*, 4th revised ed.; United Nations Publications: Geneva, 2003. Impact: insensitive >40 J, less sensitive ≥35 J, sensitive ≥4 J, very sensitive ≤3 J. Friction: insensitive >360 N, less sensitive 360 N, sensitive <360 N and >80 N, very sensitive ≤80 N, extremely sensitive ≤10 N.
(26) Köhler, J., Meyer, R., Homburg, A. *Explosivstoffe;*; Wiley-VCH: Weinheim, 2008.
(27) Klapötke, T. M. *Chemistry of High-Energy Materials*, 5th ed.; DeGruyter: Boston, 2019.
(28) Klapötke, T. M. *Energetic Materials Encyclopedia*, 1st ed.; DeGruyter: Boston, 2018.
(29) Zhang, C.; Xue, C.; Cao, Y.; Zhou, Y.; Li, H.; Zhou, J.; Gao, T. T. Intermolecular friction symbol derived from crystal information. *CrystEngComm* **2013**, *15*, 6837.
(30) Curtiss, L. A.; Raghavachari, K.; Redfern, P. C.; Pople, J. A. Assessment of Gaussian-2 and density functional theories for thecomputation of enthalpies of formation. *J. Chem. Phys.* **1997**, *106*, 1063.
(31) Byrd, E.; Rice, B. M. Improved Prediction of Heats of Formation of Energetic Materials Using Quantum Mechanical Calculations. *J. Phys. Chem. A* **2006**, *110*, 1005.
(32) Suceska, M. *Explo5 V6.05*; Brodarski Institute: Zagreb, 2018;.
(33) Klapötke, T. M.; Krumm, B.; Steemann, F. X.; Umland, K.-D. Bis(1,3-dinitratoprop-2-yl) nitramine, a new sensitive explosivecombining a nitrate ester with a nitramine. *Z. Anorg. Allg. Chem.* **2010**, *636*, 2343.
(34) *CrysAlisPro (Ver. 171.33.41)*; Oxford Diffraction Ltd.: 2009.
(35) Burla, M. C.; Caliandro, R.; Carrozzini, B.; Cascarano, G. L.; Cuocci, C.; Giacovazzo, C.; Mallamo, M.; Mazzone, A.; Polidori, G. Crystal structure determination and refinement via SIR2014. *J. Appl. Crystallogr.* **2015**, *48*, 306−309.
(36) Hübschle, C. B.; Sheldrick, G. M.; Dittrich, B. ShelXle: a graphical user interface for SHELXL. *J. Appl. Crystallogr.* **2011**, *44*, 1281−1284.
(37) Sheldrick, G. M. *SHELXL-97, Program for the Refinement of Crystal Structures*; University of Göttingen, Göttingen, Germany, 1997.
(38) Sheldrick, G. M. A short history of SHELX. *Acta Crystallogr., Sect. A: Found. Crystallogr.* **2008**, *64*, 112−122.
(39) Spek, A. L. *PLATON, A Multipurpose Crystallographic Tool*; Utrecht University: The Netherlands, 1999.
(40) Farrugia, L. J. WinGX and ORTEP for Windows: an update. *J. Appl. Crystallogr.* **2012**, *45*, 849−854.

https://dx.doi.org/10.1021/acs.cgd.0c01049
Cryst. Growth Des. XXXX, XXX, XXX−XXX